Geoscience Frontiers 11 (2020) 843–853

Contents lists available at ScienceDirect

Geoscience Frontiers

journal homepage: www.elsevier.com/locate/gsf

Research Paper

Strategies towards robust interpretations of *in situ* zircon Lu–Hf isotope analyses

C.J. Spencer [a,b,*], C.L. Kirkland [c], N.M.W. Roberts [d], N.J. Evans [e], J. Liebmann [a]

[a] School of Earth and Planetary Sciences, The Institute for Geoscience Research (TIGeR), Curtin University, Perth, Australia
[b] Department of Geological Sciences and Geological Engineering, Queen's University, Kingston, Canada
[c] Centre for Exploration Targeting – Curtin Node, The Institute for Geoscience Research, School of Earth and Planetary Sciences, Curtin University, Perth, Australia
[d] Geochronology and Tracers Facility, British Geological Survey, Nottingham, UK
[e] John de Laeter Centre GeoHistory Facility, School of Earth and Planetary Sciences, Curtin University, Perth, Australia

ARTICLE INFO

Handling Editor: M. Santosh

Keywords:
Zircon
Geochronology
Isotope geochemistry
Lu–Hf isotopes
Geostatistics
Data visualization

ABSTRACT

The combination of U–Pb and Lu–Hf compositions measured in zircon crystals is a remarkably powerful isotopic couplet that provides measures on both the timing of mineral growth and the radiogenic enrichment of the source from which the zircon grew. The U–Pb age documents the timing of zircon crystallization/recrystallization and Hf isotopes inform on the degree to which the host melt was derived from a radiogenic reservoir (e.g. depleted mantle) versus an unradiogenic reservoir (e.g. ancient continental crust), or some mixture of these sources. The ease of generating large quantities of zircon U–Pb and Lu–Hf data has been in large part facilitated by instrument advances. However, the dramatic increase in time constrained zircon Lu–Hf analyses in the Earth science community has brought to the fore the importance of careful data collection and reduction workflows, onto which robust geological interpretations may be based. In this work, we discuss the fundamentals of Lu–Hf isotopes in zircon, which then allows us to provide a robust, accessible, methodology for the assessment of data quality. Additionally, we discuss some novel techniques for: data visualization — that facilitates better transparency of data interpretation; integration of geographic information — that may reveal spatial trends where temporal trends were only apparent before; and some novel statistical evaluation tools — that may provide more rigorous inter- and intra-sample comparisons.

1. Fundamentals of Lu–Hf isotopes

The past ten years have seen a dramatic increase in Lu–Hf analyses of zircon grains (Fig. 1). Such burgeoning datasets require a data reduction workflow based around the demonstration of data quality as well as utilization of statistical tools to systematically extract information out of datasets that may be large and complex. As a prelude to discussing means of demonstrating data quality and data visualization, we provide a brief introduction to Lu–Hf systematics in zircon and discuss their utility when coupled to zircon geochronology.

2. Zircon and terrestrial isotopic compositions

Lutetium is naturally monoisotopic with one dominant radioactive isotope (^{176}Lu) forming ~3% of the total Lu with the remaining ~97% (^{175}Lu) being stable. Radioactive ^{176}Lu has a half-life of ~37.8 Ga which makes it a prime candidate as a radiogenic isotopic tracer and geochronometer of the protracted geological history of Earth. The major mode of radioactive decay of ^{176}Lu produces ^{176}Hf through beta minus decay (β^-). There are currently a number of decay constant estimates that range from ~1.7E-11/yr to ~1.96E-11/yr (Albarède et al., 2006). Although constraining the decay constant of nuclides decaying by β-emission has proven difficult, lending to a wide range of λ^{176}Lu, age comparison of terrestrial materials has yielded a more consistent λ^{176}Lu of 1.867 ± 0.013 (Scherer et al., 2001; Söderlund et al., 2004; Albarède et al., 2006). Using the decay constant, the age equation can be used to calculate the ^{176}Hf at the time of zircon formation:

$$^{176}Hf_{present} = {}^{176}Hf_{initial} + {}^{176}Lu \times (e^{\lambda t} - 1)$$

Lu–Hf isotopes in zircon are not used as a geochronometer *senso stricto*, but are generally used as an isotopic 'tracer', i.e. they are used to

* Corresponding author. School of Earth and Planetary Sciences, The Institute for Geoscience Research (TIGeR), Curtin University, Perth, Australia.
E-mail addresses: cspencer@curtin.edu.au, spenchristoph@gmail.com (C.J. Spencer).
Peer-review under responsibility of China University of Geosciences (Beijing).

https://doi.org/10.1016/j.gsf.2019.09.004
Received 5 May 2019; Received in revised form 31 August 2019; Accepted 22 September 2019
Available online 1 October 2019

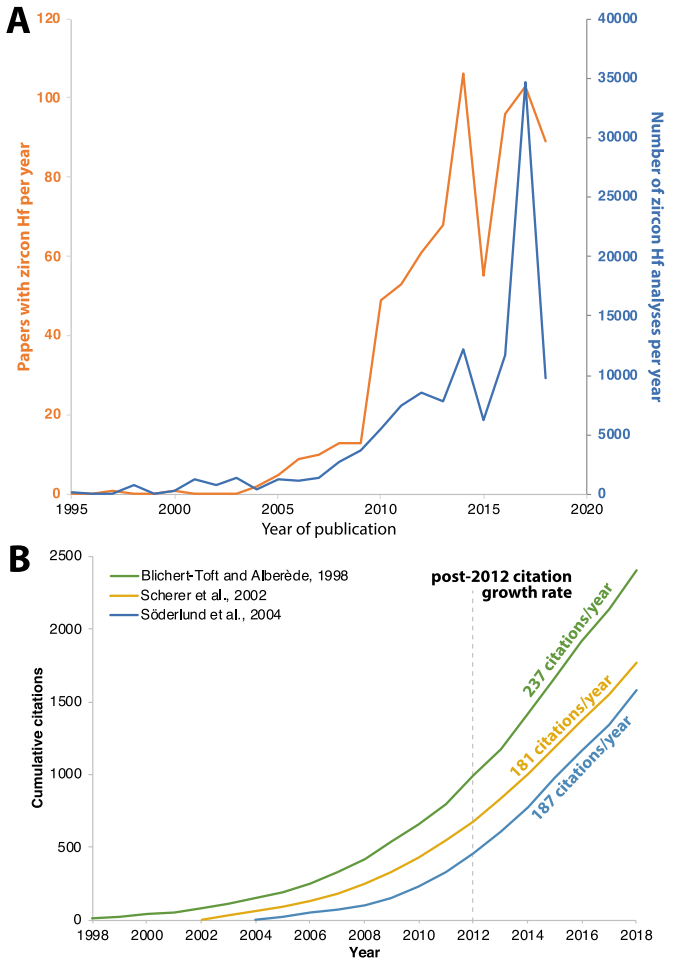

Fig. 1. (A) Orange line is number of peer-reviewed scientific publications with zircon Hf data published per year (extracted from Puetz and Condie (2019) database of ~120,000 zircon Hf analyses). Blue line is number of zircon Hf analyses from corresponding published papers. (B) Cumulative citations of three peer-reviewed studies on the Lu-decay constant of terrestrial materials. Bibliometric data gathered from Google Scholar. Post-2012 citation growth rate is constrained by linear regressions of post-2012 cumulative citation data.

trace the source of the melt that the zircon crystallised from based upon the Hf isotopic ratio. To facilitate easier comparison of Hf isotopic ratios, a general assumption is applied; the Hf isotopic composition of the bulk Earth has evolved from a source with a Lu/Hf ratio equivalent to that of chondritic meteorites (Blichert-Toft and Albarède, 1997; Fisher and Vervoort, 2018). Measured isotopic compositions are normalized to this so-called Chrondritic Uniform Reservoir (CHUR) (DePaolo and Wasserburg, 1976; Blichert-Toft et al., 1999; Vervoort et al., 1999; Patchett et al., 2004; Bouvier et al., 2008). This approach yields numbers that are larger and, in some respects, easier to compare than isotopic ratios whose significant deviation, for geological purposes, can be on the order of 100 ppm or less. The epsilon notion is used to easily visualize the isotopic composition with respect to CHUR and is calculated using the following equation:

$$\varepsilon Hf_t = \left(\frac{\frac{Hf}{Hf_{(t)}}}{\frac{Hf}{Hf_{CHUR(t)}}} - 1 \right) \times 10000$$

Estimates of the present day $^{176}Lu/^{177}Hf$ of CHUR range from 0.0332 to 0.0336 and $^{176}Hf/^{177}Hf$ range from 0.282772 to 0.282785 (Blichert-Toft and Albarède, 1997; Bouvier et al., 2008).

The other model reservoir that is used to normalize Hf measurements is Depleted Mantle. Lu and Hf are incompatible trace elements and relatively immobile. However, Hf is more incompatible (hence concentrated in the melt phase of magma) than Lu, so Hf is relatively enriched in silicates melts and the crust. Thus, a higher Lu/Hf elemental ratio (also meaning a higher $^{176}Hf/^{177}Hf$ ratio over time) is generally found in the residual solid during partial melting and removal of a liquid from the reservoir. Estimates of the isotopic composition of the present-day Depleted Mantle have varied slightly over time as more precise and more comprehensive data have become available. A recent 'best estimate' yielded a $^{176}Lu/^{177}Hf$ of 0.03976 and a $^{176}Hf/^{177}Hf$ of 0.283238 (Vervoort et al., 2018).

The wide isotopic dissimilarity between the present-day composition of CHUR and magmatic rocks derived directly from the mantle (mid-ocean ridge basalts) with highly supra-CHUR (radiogenic) values has been taken to imply that the terrestrial isotopic reservoir from which all crust was derived (i.e. the mantle) was itself formed during planetary differentiation (Vervoort and Blichert-Toft, 1999; Salters and Stracke, 2004). Using the modelled initial composition of CHUR and Depleted Mantle, the isotopic evolution of these reservoirs can be tracked through geologic time to the formation of the Earth. Previously, it has been proposed that elevated $^{142}Nd/^{144}Nd$ ratios, which in many respects are analagous to $^{176}Hf/^{177}Hf$ ratios, point to the formation of an isotopic reservoir that is depleted in incompatible elements within the first 30–75 million years following the formation of the Earth (Boyet and Carlson, 2005; Bennett et al., 2007). Furthermore, unradiogenic hafnium signatures in Hadean zircon crystals from the Jack Hills of Western Australia have been argued as evidence for a complimentary 'enriched' isotopic reservoir during the Hadean Eon (Harrison et al., 2005, 2008; Blichert-Toft and Albarède, 2008; Kemp et al., 2010; Wang and Wilde, 2018). Nevertheless, it is important to note that, despite evidence from ^{142}Nd and Hadean zircon with unradiogenic Hf compositions, the earliest excursion of Hf isotopes in mafic (and presumed mantle-derived) rocks from CHUR is proposed to have occurred at ~3.8 Ga (Fisher and Vervoort, 2018). This observation implies that global mantle differentiation and incompatible element depletion did not occur until ca. 3.8 Ga and that the unradiogenic signatures of Hadean zircon may very well be a consequence of small-scale and significantly fractionated melts.

Previous workers have also attempted to characterize other isotopic compositions in natural reservoirs. Dhuime et al. (2011) compiled the Lu–Hf isotopic composition of modern island arcs, and demonstrated that these have average compositions less radiogenic than the Depleted Mantle; the cause of this less radiogenic signature is due to contamination of mantle-derived melts from subducted sediment and assimilated crust. Dhuime et al. (2011) proposed a novel average isotopic composition of 'new crust' which they suggest should be used to calculate model ages. Nonetheless, Depleted Mantle serves as a more useful composition as it is more easily defined and, in theory, represents an end-member composition. New Crust on the other hand is the average of a very wide-range of compositions, and is not an end-member since its composition is known to arise from a mixture of sources – i.e. old sediment and crust mixed with mantle (White and Patchett, 1984; Plank, 2005; Chauvel et al., 2008).

Evaluation of $^{176}Hf/^{177}Hf$ in zircon is best placed in the context of CHUR and DM reservoirs. Just as with the evolution of CHUR and Depleted Mantle, the isotopic evolution in zircon itself is controlled by zircon $^{176}Lu/^{177}Hf$ which is extremely low. This means that any radiogenic ingrowth is minimal, and hence, the age correction to derive the initial ratio is small. However, any melt from which zircon grows will have a Lu/Hf ratio (in all likelihood) much greater than that in the zircon grain itself. The $^{176}Lu/^{177}Hf$ of terrestrial materials can be estimated using known isotopic abundances and elemental ratios:

$$Lu \Big/ Hf = \frac{Lu\ \ ppm}{Hf\ \ ppm} \times \left(\frac{Iso.wt.Lu}{Iso.wt.Hf} \times \frac{Iso.abun.Lu}{Iso.abun.Hf} \right) \times \frac{At.wt.Hf}{At.wt.Lu}$$

Table 1
Approximate conversion of εHf/Ma to $^{176}Hf/^{177}Hf$.

$^{176}Lu/^{177}Hf$	εHf/Ma
0.000	0.022
0.010	0.016
0.012	0.014
0.015	0.012
0.022	0.008
0.030	0.002

Using elemental ratios of various crustal reservoirs, the $^{176}Lu/^{177}Hf$ of the crust ranges from ~0.026 (lower continental crust) to 0.01 (upper continental crust). For ease of use, the $^{176}Lu/^{177}Hf$ evolution trajectory can be estimated as a function of εHf/Ma (Table 1) using the following equation:

$$Lu/Hf = -1.5116 \times \frac{\varepsilon Hf_{(t)}}{Ma} + 0.0337$$

The $^{176}Lu/^{177}Hf$ evolution trajectory is thus useful in calculating the time at which the $^{176}Hf/^{177}Hf$ of the sample may have been the same as various isotopic reservoirs (CHUR or Depleted Mantle).

Partial melting will preferentially partition Hf strongly into the silicate melt, whereas Lu will reside in the residuum (Lu is less incompatible). Hence, as mantle rocks contain elevated Lu they will develop $^{176}Hf/^{177}Hf$ that changes more significantly over time than crustal rocks. In contrast, crustal rocks have $^{176}Hf/^{177}Hf$ that will only change slightly from the time of mantle extraction due to low Lu content and lower Lu/Hf.

3. Measurement of isotopic compositions

Natural variations in $^{176}Hf/^{177}Hf$ are very small and there is the need for high precision in any measurement capable of addressing geological questions. Zircon has a high Hf content and low Lu content and can be readily dated. Therefore, zircon is highly suitable for $^{176}Hf/^{177}Hf$ measurement and calculation of $^{176}Hf/^{177}Hf$ initial ratios. However, there are specific analytical challenges that must be overcome. Isobaric interferences of Yb and Lu at mass 176 must be corrected for and this correction must be evaluated to ensure the interferences have been adequately dealt with (Fig. 2).

The fractionation between heavy and light isotopes needs to be

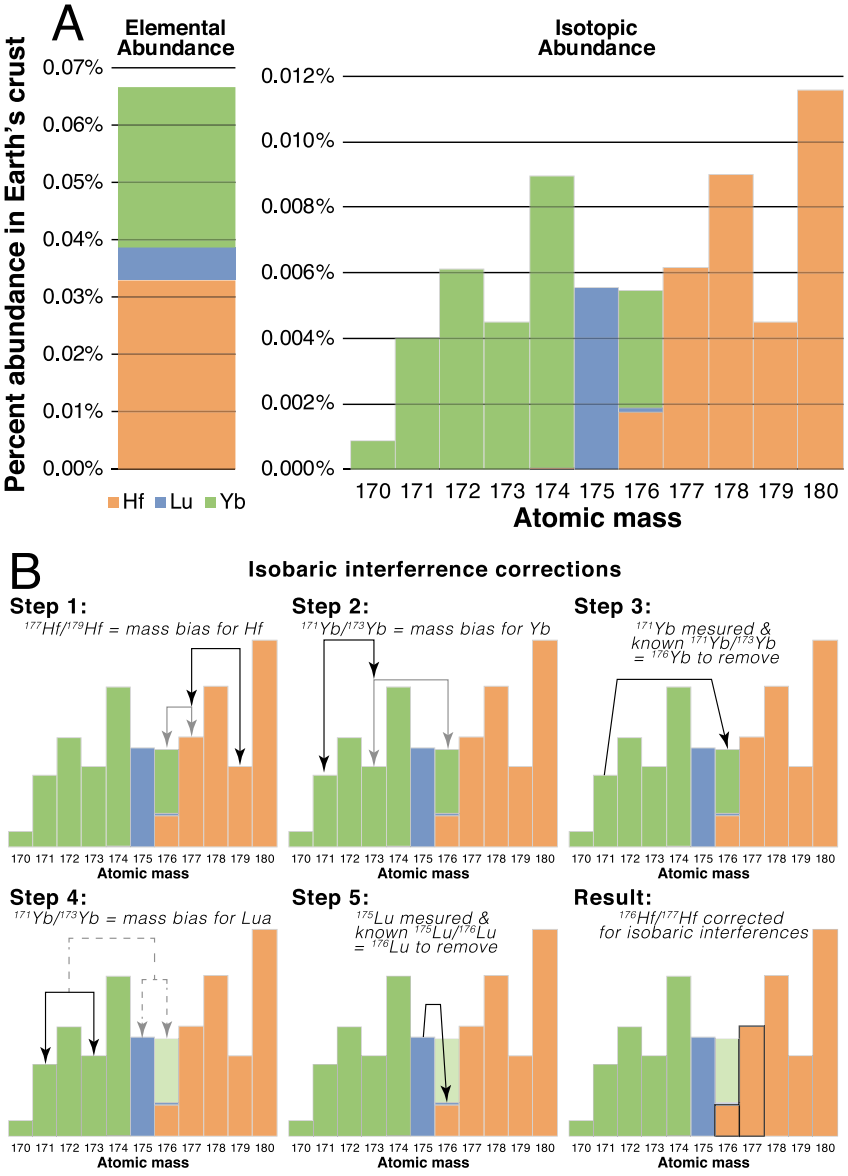

Fig. 2. (A) Elemental and isotopic abundance of Yb, Lu, and Hf in the crust (Meija et al., 2016). (B) Visualization of the five-step process of correcting isobaric interferences in Hf isotope geochemistry.

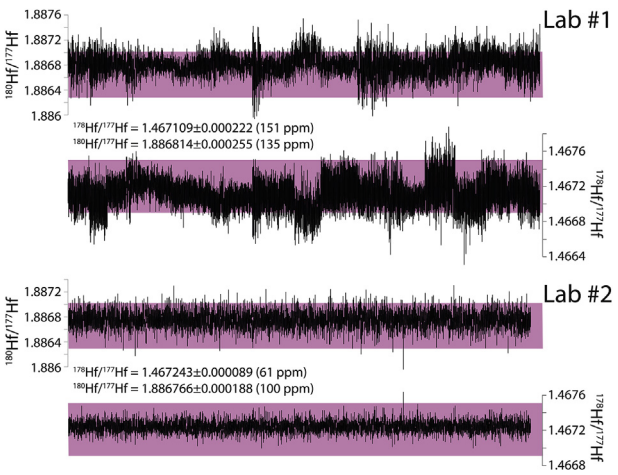

Fig. 3. Multi-year compilations (>3 years) of stable Hf isotope ratios from two separate LA-ICP-MS laboratories. The pink field represents 200 ppm variation from the predicted stable isotope ratios based upon known atomic weights and proportions.

corrected, and the effect of isobaric interferences needs to be stripped from measured ratios of interest. The $^{177}Hf/^{179}Hf$ ratio can serve as a measure of this mass bias for the Hf isotopes and a correction applied on $^{176}Hf/^{177}Hf$. This is a significant magnitude of correction. As with Hf mass bias fractionation, Yb fractionation also needs to be measured and corrected. Typically, $^{171}Yb/^{173}Yb$ will be measured and a correction factor determined, which in most cases is also substantial (>1%/atomic mass unit). A fractionation-corrected $^{173}Yb/^{176}Yb$ signal can then be calculated. The calculated ^{176}Yb (fractionation-corrected) needs to be removed from the ^{176}X signal, which can be accomplished by measuring ^{171}Yb, applying the determined mass bias correction and using a known fixed $^{171}Yb/^{176}Yb$ ratio. The remaining isobaric interference on ^{176}Hf now is only from ^{176}Lu. Lu has two isotopes (^{175}Lu and ^{176}Lu) so it is not possible to directly measure a mass bias. Therefore, fractionation of Lu is assumed to be equivalent to fractionation of Yb. Fortunately, Lu interference on ^{176}X is minimal so if this assumption is inaccurate, it has little effect on calculated final $^{176}Hf/^{177}Hf$ ratio. The fraction-corrected $^{175}Lu/^{176}Lu$ ratio is used to calculate the abundance of ^{176}Hf free of ^{176}Lu interference. As can be appreciated from this preamble, correction for mass basis and interference is non-trivial and a range of strategies is presented to demonstrate that a correction approaches efficacy.

4. Zircon Lu–Hf workflow

4.1. Assessment of stable Hf isotopes

The Hf isotopic system benefits from the existence of several stable isotopes (e.g. ^{177}Hf, ^{178}Hf, ^{180}Hf). Hence the stable isotope ratios can provide a useful measure of confidence in instrument stability and the accuracy of mass bias corrections. Based upon known atomic weights and proportions, the $^{178}Hf/^{177}Hf$ and $^{180}Hf/^{177}Hf$ are 1.46717 and 1.88666, respectively (Blichert-Toft and Albarède, 1997). Long term analysis of Hf isotopes via inductively-coupled plasma mass spectrometry (ICP-MS) indicates long term reproducibility with ~200 ppm, with reproducibility being calculated with the following equation:

$$\text{reproducibility (ppm)} = \frac{\text{standard deviation}}{\text{average}} \times 10^6$$

Multi-year compilations (>3 years) of stable Hf isotope ratios from two different laboratories running different mass spectrometers and laser ablation systems provide a useful benchmark to compare future Hf studies. We consider analyses that lie within 200 ppm of the natural stable ratios to be a useful indication that the instrument is performing adequately. This corresponds to $^{178}Hf/^{177}Hf$ between 1.46746 and 1.46688 and $^{180}Hf/^{177}Hf$ between 1.88704 and 1.88628 (Fig. 3). Analyses outside of these acceptable ranges may suffer inaccurate mass bias corrections or other unforeseen aberrations in the resulting data.

4.2. Assessment of isobaric corrections

Accurate radiogenic Hf isotope measurement requires a number of isobaric interference corrections. These corrections include the removal of ^{176}Yb and ^{176}Lu from the measured 176 mass. While there are a range of strategies to accomplish this correction (Thirlwall and Walder, 1995; Nowell and Parrish, 2001; Xu et al., 2004; Iizuka and Hirata, 2005; Wu et al., 2006; Blichert-Toft, 2008; Fisher et al., 2014), the evaluation of the resultant corrected $^{176}Hf/^{177}Hf$ ratio (and εHf) is facilitated through

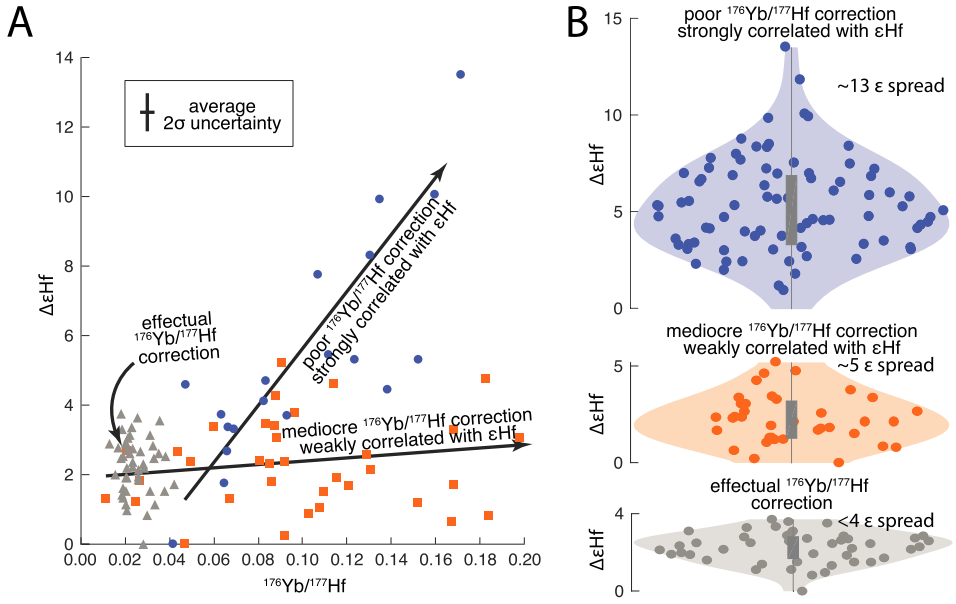

Fig. 4. (A) Three examples of real Hf isotopic data (normalized to arbitrary εHf) and the associated $^{176}Yb/^{177}Hf$ values, ranging from strongly correlated to uncorrelated. This relationship is a direct reflection of ineffectual isobaric interference correction. (B) Violin plots of probability frequency of εHf for the same samples. Greater variance is seen in the samples that display a correlation between the $^{176}Yb/^{177}Hf$ and εHf.

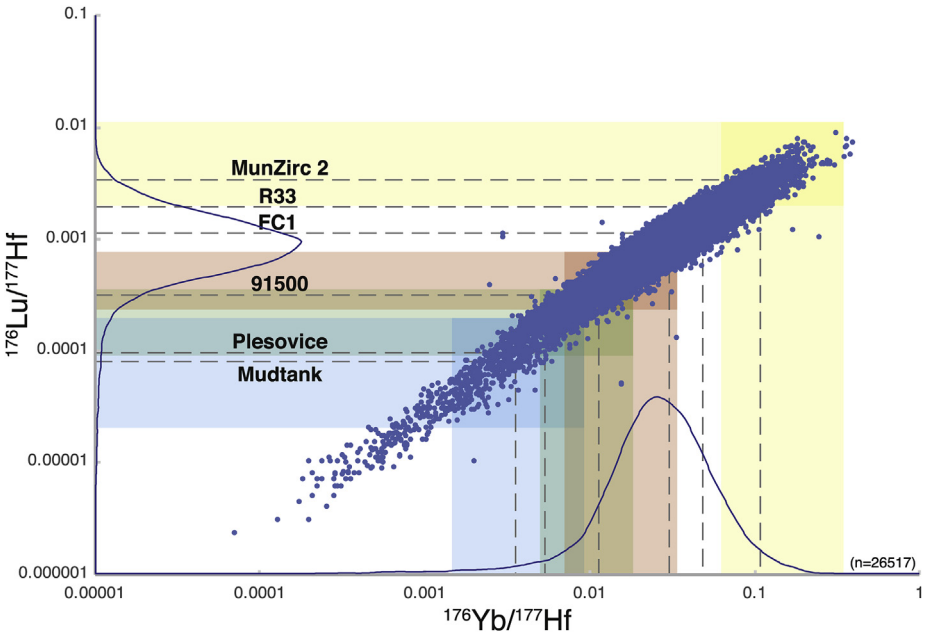

Fig. 5. Compilation of natural zircon analyses (blue spots) of $^{176}Yb/^{177}Hf$ versus $^{176}Lu/^{177}Hf$. Frequency of $^{176}Yb/^{177}Hf$ and $^{176}Lu/^{177}Hf$ are shown as probability density curves along the axes (Spencer et al., 2017). Ranges of reference material compositions are shown in colored bars for Mudtank, Plesovice, 91500, MunZirc2 (Woodhead and Hergt, 2005; Morel et al., 2008; Sláma et al., 2008; Fisher et al., 2011, 2014) as analysed by multiple laboratories over a multi-year period of time. Published median values for Mudtank, Plesovice, 91500, FC1, R33, MunZirc2 are shown in dashed lines.

assessment of the correlation between $^{176}Hf/^{177}Hf$ and $^{176}Yb/^{177}Hf$ or $^{176}Lu/^{177}Hf$ (Fig. 4). A correlation may imply an ineffectual isobaric interference correction. A shift of ~0.1 in the $^{176}Yb/^{177}Hf$ ratio can result in a change of the εHf value by > 10 epsilon units, making the accurate interpretation of any such affected data impossible.

Analysis of a range of reference materials with varying $^{176}Lu/^{177}Hf$ and $^{176}Yb/^{177}Hf$ ratios provides a useful means of validating isobaric interference corrections. Similar to other elemental and isotopic measurements, it is important that the composition of the reference material brackets that of the unknowns. The range of compositions shown in Fig. 5 allows for the appropriate reference materials to be selected based on the composition of the unknown material. A compilation of ~26,000 analyses (Roberts and Spencer, 2015) demonstrates the vast majority of natural zircon have $^{176}Lu/^{177}Hf$ between 0.0001 and 0.002 and $^{176}Yb/^{177}Hf$ between 0.008 and 0.2 (Fig. 5). This range of isotopic compositions can be encompassed by using Mudtank or Plešovice (Jackson et al., 2004; Sláma et al., 2008) on the lower isotopic side and R33 or the Memorial University synthetic zircon (doped with Yb) on the higher side (Fisher et al., 2011, 2014). We also suggest that a selected reference material should match the mode of unknown zircon composition for robustness.

4.3. Calculating εHf uncertainty

When estimating the uncertainty of any measurement, it is important to identify all of the possible sources of uncertainty including random (analytical) and systematic (Horstwood et al., 2016). Given the time-integrated nature of $^{176}Hf/^{177}Hf_{(t)}$ and $\varepsilon Hf_{(t)}$, it is important to consider the age uncertainty in conjunction with the Hf isotopic uncertainty. In a scenario where the age uncertainty is considered, the time-integrated uncertainty will broadly form a rhombus-shaped or elliptical envelope with vertical age-constraints and sloped connecting lines constrained by the $^{176}Lu/^{177}Hf$ of the zircon analysis. However, in practice, we suggest simply using the maximum and minimum $^{176}Hf/^{177}Hf_{(t)}$ or $\varepsilon Hf_{(t)}$ of the time-integrated uncertainty in conjunction with the age uncertainty (Fig. 6). Although this approach likely over-estimates the $^{176}Hf/^{177}Hf_{(t)}$ and $\varepsilon Hf_{(t)}$ uncertainty, we prefer this conservative approach when defining specific fields of similar Hf isotopic compositions (Spencer et al., 2019b). For instance, incorporating the crystallization age uncertainty (~2% age uncertainty from LA-ICPMS data) produces Hf isotope uncertainties that are ~50% larger, on average, than estimates that do not consider crystallization age and time-integrated uncertainty.

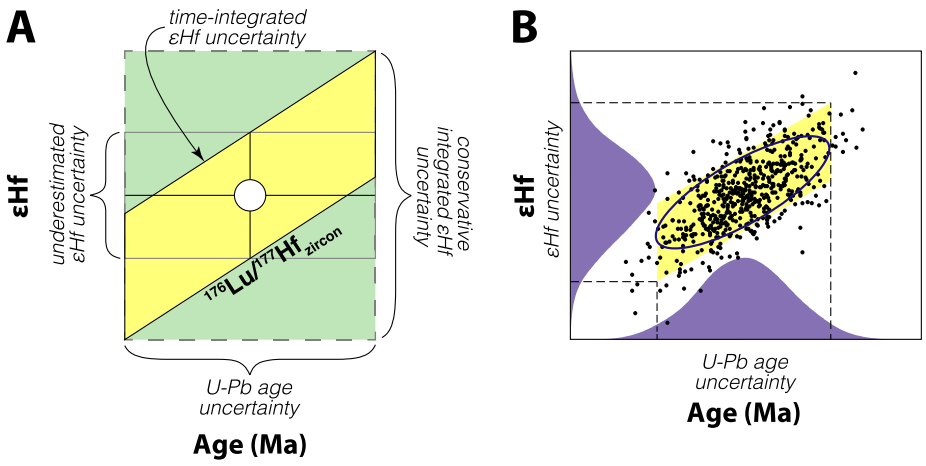

Fig. 6. (A) Schematic diagram of various ways to constrain εHf uncertainties providing a time-integrated, conservative, and underestimated εHf uncertainty. (B) Idealized representation of correlated uncertainty between εHf and age. Dashed lines represent two standard deviations in age and Hf composition.

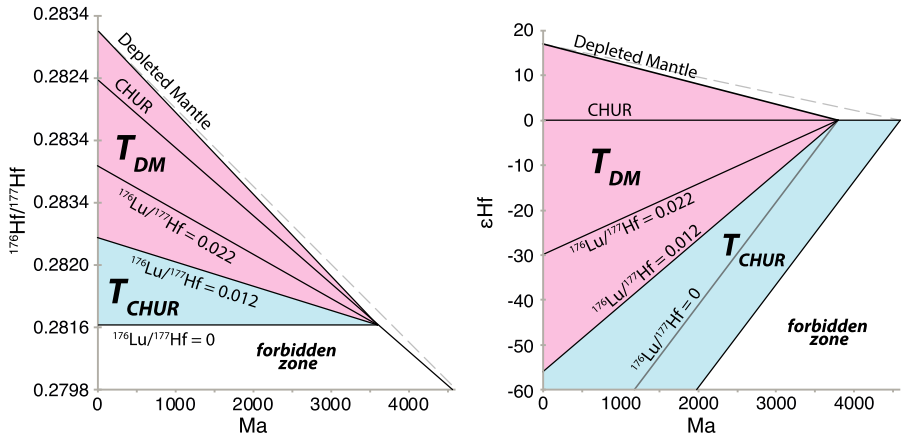

Fig. 7. Evolution of Hf isotopes shown in $^{176}Hf/^{177}Hf$ and εHf through time. Large-scale mantle depletion is hypothesized to have occurred at ~3.8 Ga (Fisher and Vervoort, 2018) and therefore Depleted Mantle model ages greater than ~3.8 Ga are likely overestimates of mantle melting.

4.4. Utility of model ages

Theorized isotopic reservoirs can be used as reference frames within which isotopic enrichment or depletion can be compared. In general, CHUR has become the most useful reference frame through the epsilon notation. Those data that have a supra-CHUR composition can be characterized as more radiogenic (i.e. there is elevated ^{176}Hf produced from a source with greater Lu than CHUR) whereas the sub-CHUR composition is unradiogenic (i.e. there is less ^{176}Hf produced from a source with less Lu than CHUR). Additionally, the Depleted Mantle can be a useful reference frame that allows for interpretations to integrate planetary differentiation and isotopic depletion of the mantle. The ability to track the $^{176}Hf/^{177}Hf$ isotopic composition of the Depleted Mantle through geologic time allows for the calculation of 'Depleted Mantle model ages' or the average 'age' of Depleted Mantle extraction. These are two stage model ages which project back in time from the present to zircon crystallization age using the $^{176}Lu/^{177}Hf$ ratio of the zircon and then in the stage prior to zircon growth using a chosen average crustal $^{176}Lu/^{177}Hf$ ratio. The limitations and utility of these model ages has been discussed at length elsewhere (Arndt et al., 1987; Roberts and Spencer, 2015; Payne et al., 2016; Vervoort and Kemp, 2016). Suffice it to say that Depleted Mantle model ages are generally not 'ages' of geologic events, but are numerical estimates of average mantle extraction ages. Only in rare cases can it be demonstrated through independent means that model age tracks a real crust production episode (Kemp et al., 2006; Nebel et al., 2007; Kirkland et al., 2013; Vervoort and Kemp, 2016). Hence, in most cases model ages should not be used to define the timing of geologic events as they rely on assumptions about the composition of parental material. Based on these assumptions, model ages then provide an indication of the potential age of the parent material. Using the isotopic estimates of the Depleted Mantle discussed above (Vervoort et al., 2018) and the timing of global mantle depletion at ~3.8 Ga (Fisher and Vervoort, 2018) we can state that, depending on the timing of mantle extraction and degree of radiogenic enrichment, either Depleted Mantle model ages (T_{DM}) or CHUR model ages (T_{CHUR}) are most appropriate when considering a specific data set (Fig. 7). For zircon with a Hf isotopic composition above the average crustal $^{176}Lu/^{177}Hf$ evolution trajectory that projects from 3.8 Ga (the timing of mantle depletion), Depleted Mantle model ages are appropriate. Conversely, for zircon with a Hf isotopic composition below the average crustal isotopic evolution trajectory, CHUR model ages are appropriate simply because Depleted Mantle extraction may have not yet occurred on the evolving planet.

4.5. Evaluating crustal evolution trajectories

Radiogenic ingrowth over time leads to linear arrays on hafnium evolution plots. In addition, isotopic evolution slopes are controlled by age. Hence, a well constrained age for initial isotopic ratio calculation (i.e. $^{176}Lu/^{177}Hf$) is critical. The slope of isotopic evolution arrays can, therefore, provide important information regarding the nature of the source material and the long-term history of the isotopic system. Plots of $^{176}Hf/^{177}Hf$ versus zircon crystallization age provide a useful indication of whether the slope of the isotopic evolution array can be explained by crustal reworking, Depleted Mantle input, mixtures of these sources, or Pb-loss having affected the age used in initial calculations. A trend attributed to Pb-loss will be (near) horizontal when displayed in $^{176}Hf/^{177}Hf$ versus age space. This Pb loss array would correspond to a $^{176}Lu/^{177}Hf$ ratio of zero, and plot as a steep trend in εHf versus age space but may be difficult to distinguish from natural compositional trends on a εHf plot. It is commonly assumed that an isotopic composition of $^{176}Lu/^{177}Hf$ between 0.010 and 0.015 approximates the isotopic evolution of the average continental crust (Vervoort and Blichert-Toft, 1999; Griffin et al., 2002; Roberts et al., 2013). Mafic lithologies will have $^{176}Lu/^{177}Hf$ greater than the average continental crust, and felsic lithologies will have a lower ratio. When converted to εHf, the isotopic evolution array will correspond to an εHf/Ma slope. Although a $^{176}Lu/^{177}Hf$ ratio of zero (i.e. as expected for Pb-loss) corresponds to an εHf/Ma slope of 0.022, determination of Pb-loss is most easily facilitated using a $^{176}Hf/^{177}Hf$ versus age plot (not εHf versus age). The slopes of linear regressions of εHf/Ma can be used to estimate the $^{176}Lu/^{177}Hf$ of the source using the equation discussed above.

Important discussions regarding the interpretation of the $^{176}Lu/^{177}Hf$ ratio and crustal evolution trajectories in complex dataset that often exhibit radiogenic Pb-loss are presented elsewhere (Griffin et al., 2004; Laurent and Zeh, 2015; Payne et al., 2016; Vervoort and Kemp, 2016).

Although the εHf/Ma slope and corresponding $^{176}Lu/^{177}Hf$ ratio are most generally used to define the isotopic evolution trajectory and interpreted to be controlled by the composition of the host rocks, it has been proposed this slope can also be used to infer changes in the geodynamic environment responsible for the crustal reworking (Spencer et al., 2018). For example, a εHf/Ma slope that corresponds to a negative (and therefore implausible) $^{176}Lu/^{177}Hf$ ratio may simply be indicative of collisional orogenesis where the reworking of progressively older crust leads to a steepened εHf/Ma slope (Kohanpour et al., 2019).

5. Interpretive strategies

5.1. Violin plots

It is often the case that zircon Hf ratios yield a range of isotopic values despite being from a single igneous sample with robust isobaric interference corrections and a single U–Pb crystallization age (Andersen et al., 2002; Griffin et al., 2002; Roberts et al., 2013; Hartnady et al., 2019). This variance of composition has been explained as being due to disequilibrium

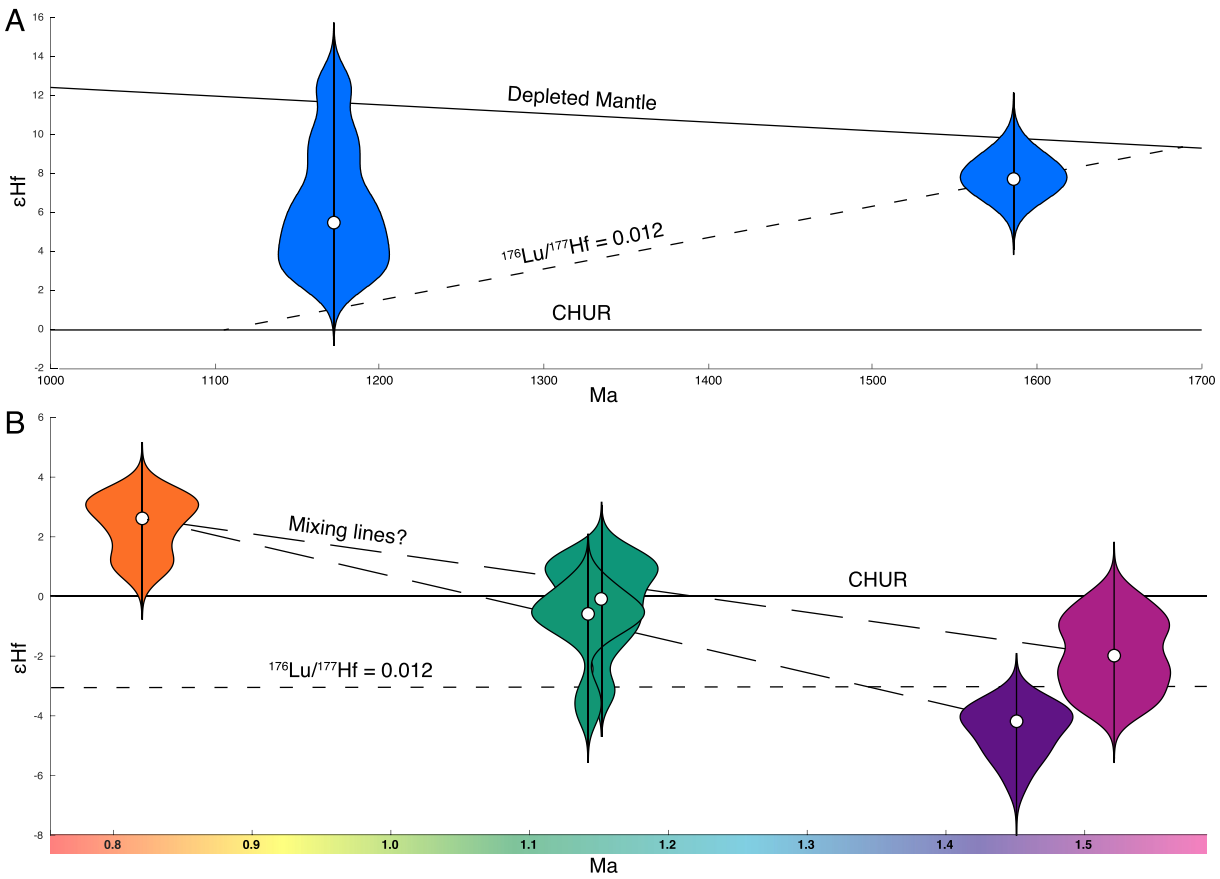

Fig. 8. Example of violin plots on various timescales. (A) Zircon Hf data from a ~1180 Ma volcanic unit with ~1600 Ma inherited zircon (de Gromard et al., 2016). Range of εHf values of the younger population implies a degree of mixing between the Depleted Mantle and the isotopically evolved composition of the older population. The distribution of data of the younger population implies that mixing of the old crust was greater than that of the Depleted Mantle. (B) Zircon Hf data from a young plutonic system showing changes in the isotopic signature (increasing mantle component) on < 1 Myr timescales (Spencer et al., 2019a).

of the magma composition (Villaros et al., 2009; Tang et al., 2014) or magma mixing (Griffin et al., 2002; Belousova et al., 2006; Kemp et al., 2007). Regardless of the petrological reason for the wide range of zircon εHf compositions within a single magmatic system, the visualization of such data generally cannot be effectively accomplished via a simple arithmetic, geometric, or weighted mean (±2 standard deviations). For weighted means, it is important to evaluate the reduced chi-squared statistic (mean square weighted deviation, MSWD) and whether or not the data display over- or under-dispersion (Spencer et al., 2016). Many scholars make use of histograms or probability density functions; however these diagrams do not allow for the samples to be placed in their temporal context. For this reason, a useful tool for displaying Hf data is a violin plot, where the distribution of εHf is displayed as a vertical density function mirrored on the vertical axis and placed in its proper temporal location along the horizontal axis (Fig. 8). This approach provides a means to clearly show data frequency and the range of isotopic compositions, while simultaneously correctly showing the temporal context. Violin plots can be constructed using a variety of software packages (Python, Matlab, Plotly, BoxPlotR). See supplementary methods for further information.

5.2. Data density plots

When displaying large compiled databases of zircon Hf data, scatterplots are often used to visualize the data. However, these diagrams cannot quantitatively treat data density. In 1-dimensional distributions (such as detrital zircon age spectra), kernel density estimations have proven to be useful to provide a relative likelihood of different ages in the population (Botev et al., 2010; Vermeesch, 2012). In most cases, the kernel density estimation simply adds gaussian curves (the kernel) of a given bandwidth to form a single smooth curve. The selection of the bandwidth is important as this will control the smoothness of the curve. If the bandwidth is too narrow, then the distribution will be under-smoothed and may give an invalid perception of the frequency of meaningful age populations (showing a single age population as multiple peaks). If the bandwidth is too wide, it will mask multiple age populations within a single peak. While there are a number of strategies for choosing the most appropriate bandwidth (Vermeesch, 2012), we recommend that the kernel density bandwidth is set to meet the fundamental limitations of the analytical equipment used (i.e., average zircon age uncertainty).

The same kernel density estimation approach can be accomplished in two dimensions with zircon U–Pb and εHf to create a bivariate kernel density estimation diagram (Fig. 9) (Botev et al., 2010; Spencer et al., 2019b). Importantly, the kernel density estimation algorithm should use independent bandwidths for U–Pb and εHf (e.g., 20 Ma for U–Pb and 1 epsilon unit for εHf, or the average age and εHf uncertainties; Spencer et al., 2019b).

5.3. Hf isotopic mapping

The Nd isotope system has long been used to track crustal evolution. A powerful way of visualising such information has been to contour initial ratios or model ages to produce maps that may track zones of reworking or enhanced mantle input (Milisenda et al., 1988, 1994; Herrell et al., 2006; Dickin and Strong, 2019) and may delineate metallogenic tracks (Cassidy et al., 2004; Champion and Cassidy, 2007; Wyche et al., 2012). More recently, the Hf isotope system has been utilised in a similar way but with some important advantages (Kirkland et al., 2011; Mole et al., 2015). Each Hf isotope analysis of zircon may be time constrained with its U–Pb age,

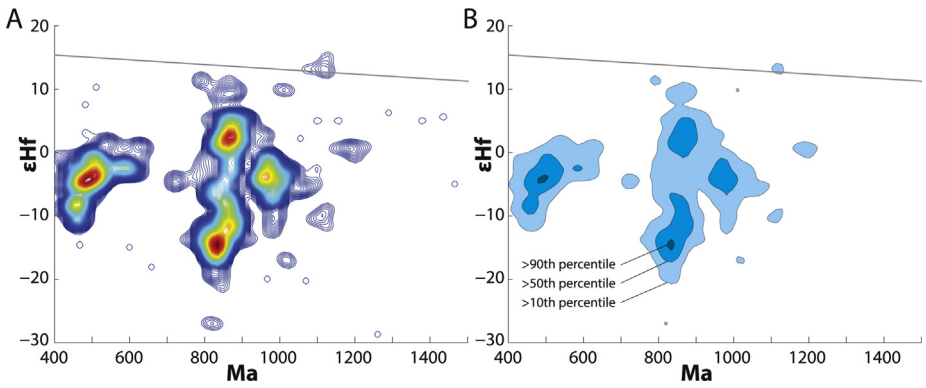

Fig. 9. (A) Example of bivariate kernel density estimation 2dKDE of εHf and U–Pb zircon data (Spencer et al., 2019b). Bandwidth of U–Pb is 20 million years and 1 epsilon for εHf. (B) Simplified 2dKDE by showing the 10th, 50th, 90th percentiles (contours of increasing data density).

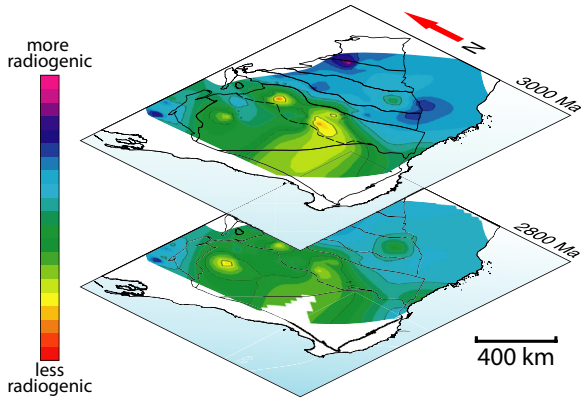

Fig. 10. Nearest neighbor interpolation of zircon Hf Depleted Mantle model ages (T_{DM}) in southern Western Australia shown in two time slices representing the spatial distribution of magmatism at ~2800 Ma and ~3000 Ma (Kirkland et al., 2011). Note arrow highlighting early development of possible rift zone in the north west Yilgarn (refer to Supplementary Fig. 2).

removing ambiguity in initial ratio determination in whole rock Nd approaches. Furthermore, as each analysis of zircon has an associated location and an age, the Hf isotopic signature can be used to develop time dynamic images of the development of crust (Fig. 10). On many occasions, each specific location within a Hf isotopic map can be constrained at different points in time, with associated unique Hf ratios, as samples may contain older inherited zircons. While such inherited zircon may blur the spatial resolution, they do provide further temporal resolution. There are several approaches to collating data sets suitable for Hf isotopic mapping, the most common being age bin averaging, where the median of isotopic values for each sample for a given age range is computed and the median value spatially interpolated between different sample locations. The age span of the bin can be changed with pay offs in terms of sample density versus temporal resolution. Isotopic maps have been produced for both initial ratios and model ages. Many interpolation and approximation methods have been developed to predict values of spatial phenomena in unsampled locations (Franke, 1982; Lam, 1983; Burrough, 1986; McCullagh, 1988; Franke and Nielson, 1991; Watson, 1999) and this is readily accomplished in GIS applications. One widely used approach in Hf isotopic mapping is inverse distance weighting, which assumes that the value at an unsampled point can be approximated as a weighted average of values at points within a certain cut-off distance, or from a given number m of the closest points (typically 15). Weights are usually inversely proportional to a power of distance (Burrough, 1986; Watson, 1999) which, at an unsampled location, leads to an estimator. In the case of time dynamic maps (e.g. animated maps), it is feasible to implement between bin morphing, where the calculated isotopic grid is morphed into the next age bin grid over a number of temporal steps. Basically, this approach is temporal interpolation as opposed to spatial interpolation and is carried out between two end-member grids to yield an animation showing how the isotopic parameter may have changed over both space and time.

It should be remembered that such visualization techniques, although based on measured data, are still only models as they necessitate assumptions in both spatial and temporal dimensions. An animation of the temporal change between 3.0 Ga and 2.2 Ga in two-stage Depleted Mantle model ages across the Yilgarn Craton, Western Australia, is presented in Supplementary Fig. 2 produced from a compilation of available zircon Hf isotopic data in the region. The Hf isotopic pattern reveals breaks and gradients that correspond to known zones of mineralization, including gold, and the location of Komatiite volcanism (Mole et al., 2015). A distinct feature of this animation is the development of the relatively more juvenile Eastern Goldfield Superterrane across the Ida Fault and an earlier juvenile mantle corridor running NNE–SSW, developing at 3.0 Ga, between the towns of Que and Meekatharra, where several large vanadium bearing ca. 2.8 Ga mafic bodies are concentrated (Ivanic et al., 2010).

6. Conclusions

Hf isotopes allow a wide range of geological questions to be addressed, such as, what is the proportion of magmatic addition from the mantle to the crust? How does the source of magma change over time? Where are major crustal structures? Furthermore, due to the ability to delineate major crustal structures, spatial relationships in isotopic signatures can have metallogenic significance. Despite the clear power of time constrained Hf isotopes to address questions on crustal evolution, measurement of Hf isotopes in zircon is non-trivial, requiring five corrections for mass bias and interference to allow meaningful $^{176}Hf/^{177}Hf$ ratios to be calculated. Additionally, the precision of measurement needed to address geological questions necessitates accurate measurement to the 5th decimal place.

The work flow that is presented in this study (Inline Supplementary Fig. S1), provides a baseline to help assure that the steps taken towards data correction and interpretation are robust and rooted in fundamental geologic, isotopic, and analytical constraints. This workflow in no way represents the only method through which Hf isotopes of zircon can be interpreted, but merely provides suggestions towards our view of best practice.

Acknowledgements

GeoHistory Facility instruments in the John de Laeter Centre, Curtin University, Autralia, were funded via an Australian Geophysical Observing System grant provided to AuScope Pty Ltd. by the AQ44 Australian Education Investment Fund program. The NPII multi-collector was obtained via funding from the Australian Research Council LIEF program (LE150100013).

Appendix

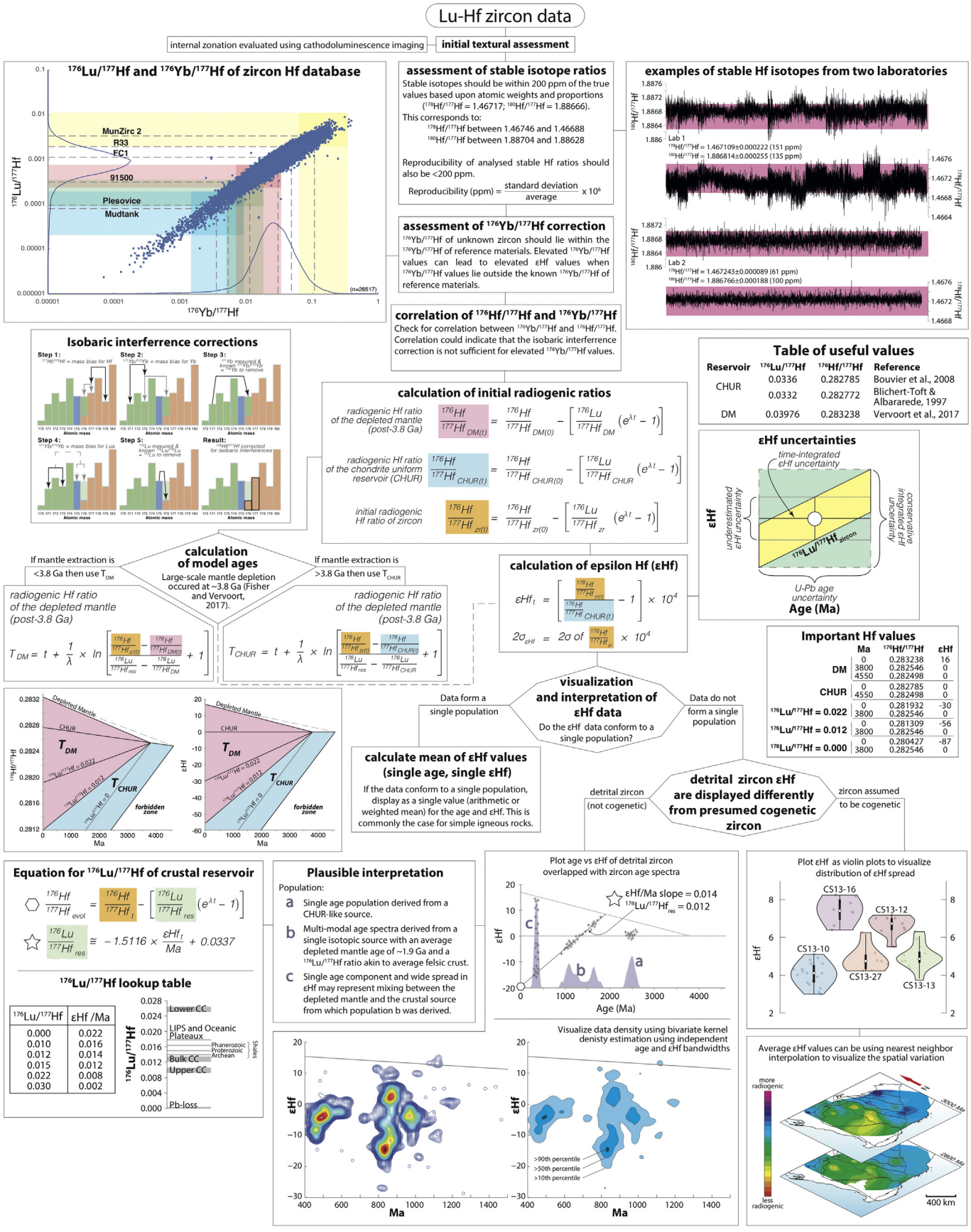

Inline Supplementary Figure S1. Flowchart outlining the recommended workflow from reduced and corrected Lu–Hf zircon data to interpretable results.

Appendix A. Supplementary data

Supplementary data to this article can be found online at https://doi.org/10.1016/j.gsf.2019.09.004.

References

Albarède, F., Scherer, E.E., Blichert-Toft, J., Rosing, M., Simionovici, A., Bizzarro, M., 2006. γ-ray irradiation in the early Solar System and the conundrum of the ^{176}Lu decay constant. Geochem. Cosmochim. Acta 70, 1261–1270.

Andersen, T., Griffin, W.L., Pearson, N.J., 2002. Crustal evolution in the SW part of the Baltic Shield: the Hf isotope evidence. J. Petrol. 43, 1725–1747.

Arndt, N.T., Goldstein, S.L., 1987. Use and abuse of crust-formation ages. Geology 15 (10), 893–895.

Belousova, E.A., Griffin, W.L., O'Reilly, S.Y., 2006. Zircon crystal morphology, trace element signatures and Hf isotope composition as a tool for petrogenetic modelling: examples from Eastern Australian granitoids. J. Petrol. 47, 329–353.

Bennett, V.C., Brandon, A.D., Nutman, A.P., 2007. Coupled ^{142}Nd-^{143}Nd isotopic evidence for Hadean mantle dynamics. Science Am. Assoc. Adv. Sci. 318, 1907–1910.

Blichert-Toft, J., 2008. The Hf isotopic composition of zircon reference material 91500. Chem. Geol. 253, 252–257.

Blichert-Toft, J., Albarède, F., 1997. The Lu-Hf isotope geochemistry of chondrites and the evolution of the mantle-crust system. Earth Planet. Sci. Lett. 148, 243–258.

Blichert-Toft, J., Albarède, F., 2008. Hafnium isotopes in Jack Hills zircons and the formation of the Hadean crust. Earth Planet. Sci. Lett. 265, 686–702.

Blichert-Toft, J., Gleason, J.D., Télouk, P., Albarède, F., 1999. The Lu–Hf isotope geochemistry of shergottites and the evolution of the Martian mantle–crust system. Earth Planet. Sci. Lett. 173, 25–39.

Botev, Z.I., Grotowski, J.F., Kroese, D.P., 2010. Kernel density estimation via diffusion. Ann. Stat. 38, 2916–2957.

Bouvier, A., Vervoort, J.D., Patchett, P.J., 2008. The Lu-Hf and Sm-Nd isotopic composition of CHUR: constraints from unequilibrated chondrites and implications for the bulk composition of terrestrial planets. Earth Planet. Sci. Lett. 273, 48–57.

Boyet, M., Carlson, R.W., 2005. Geochemistry: ^{142}Nd evidence for early (>4.53 Ga) global differentiation of the silicate earth. Science Am. Assoc. Adv. Sci. 309, 576–581.

Burrough, P.A., 1986. Principles of Geographical. Information Systems for Land Resource Assessment. Clarendon Press, Oxford.

Cassidy, K.F., Champion, D.C., Muhling, J., Knox-Robinson, C.M., 2004. Crustal evolution of the Yilgarn Craton from Nd isotopes and granite geochronology: implications for metallogeny. SEG 317–320.

Champion, D.C., Cassidy, K.F., 2007. An overview of the Yilgarn Craton and its crustal evolution. Rec. Geosci. Aust. 14, 8–13.

Chauvel, C., Lewin, E., Carpentier, M., Arndt, N.T., Marini, J.-C., 2008. Role of recycled oceanic basalt and sediment in generating the Hf–Nd mantle array. Nat. Geosci. 1, 64.

de Gromard, R.Q., Wingate, M.T.D., Kirkland, C.L., Smithies, R.H., Howard, H.M., 2016. Geology and U-Pb Geochronology of the Warlawurru Supersuite and MacDougall Formation in the Mitika and Wanarn Areas, West Musgrave Province. Geological Survey of Western Australia.

DePaolo, D.J., Wasserburg, G.J., 1976. Inferences about magma sources and mantle structure from variations of ^{143}Nd/^{144}Nd. Geophys. Res. Lett. 3, 743–746.

Dhuime, B., Hawkesworth, C., Cawood, P., 2011. When continents formed. Science 331, 154–155.

Dickin, A.P., Strong, J.W.D., 2019. Nd isotope mapping of the Grenvillian Allochthon boundary thrust in Algonquin park, Ontario. Can. J. Earth Sci. 56, 101–110.

Fisher, C.M., Hanchar, J.M., Samson, S.D., Dhuime, B., Blichert-Toft, J., Vervoort, J.D., Lam, R., 2011. Synthetic zircon doped with hafnium and rare earth elements: a reference material for in situ hafnium isotope analysis. Chem. Geol. 286, 32–47.

Fisher, C.M., Vervoort, J.D., 2018. Using the magmatic record to constrain the growth of continental crust—the Eoarchean zircon Hf record of Greenland. Earth Planet. Sci. Lett. 488, 79–91.

Fisher, C.M., Vervoort, J.D., Hanchar, J.M., 2014. Guidelines for reporting zircon Hf isotopic data by LA-MC-ICPMS and potential pitfalls in the interpretation of these data. Chem. Geol. 363, 125–133.

Franke, R., 1982. Scattered data interpolation: tests of some methods. Math. Comput. 38, 181–200.

Franke, R., Nielson, G.M., 1991. Scattered Data Interpolation and Applications: A Tutorial and Survey. In: Hagen, H., Roller, D. (Eds.), Geometric Modeling. Computer Graphics — Systems and Applications. Springer, Berlin, Heidelberg.

Griffin, W.L., Belousova, E.A., Shee, S.R., Pearson, N.J., O'Reilly, S.Y., 2004. Archean crustal evolution in the northern Yilgarn Craton: U-Pb and Hf-isotope evidence from detrital zircons. Precambrian Res. 131, 231–282.

Griffin, W.L., Wang, X., Jackson, S.E., Pearson, N.J., O'Reilly, S.Y., Xu, X., Zhou, X., 2002. Zircon chemistry and magma mixing, SE China: In-Situ analysis of Hf isotopes, Tonglu and Pingtan Igneous Complexes, 61. Lithos, pp. 237–269.

Harrison, T.M., Blichert-Toft, J., Müller, W., Albarede, F., Holden, P., Mojzsis, S.J., 2005. Heterogeneous Hadean hafnium: evidence of continental crust at 4.4 to 4.5 Ga. Science 310, 1947–1950.

Harrison, T.M., Schmitt, A.K., McCulloch, M.T., Lovera, O.M., 2008. Early (≥ 4.5 Ga) formation of terrestrial crust: Lu-Hf, δ^{18}O, and Ti thermometry results for Hadean zircons. Earth Planet. Sci. Lett. 268, 476–486.

Hartnady, M.I.H., Kirkand, C.L., Smithies, R.H., Poujol, M., Clark, C., 2019. Periodic Paleoproterozoic calc-alkaline magmatism at the south eastern margin of the Yilgarn Craton; implications for Nuna configuration. Precambrian Res. 105400.

Herrell, M.K., Dickin, A.P., Morris, W.A., 2006. A test of detailed Nd isotope mapping in the Grenville Province: delineating a duplex thrust sheet in the Kipawa Mattawa region. Can. J. Earth Sci. 43, 421–432.

Horstwood, M.S.A., Košler, J., Gehrels, G., Jackson, S.E., McLean, N.M., Paton, C., Pearson, N.J., Sircombe, K., Sylvester, P., Vermeesch, P., Bowring, J.F., Condon, D.J., Schoene, B., 2016. Community-derived standards for LA-ICP-MS U-(Th-)Pb geochronology – uncertainty propagation, age interpretation and data reporting. Geostand. Geoanal. Res. 40, 311–332.

Iizuka, T., Hirata, T., 2005. Improvements of precision and accuracy in in situ Hf isotope microanalysis of zircon using the laser ablation-MC-ICPMS technique. Chem. Geol. 220, 121–137.

Ivanic, T.J., Wingate, M.T.D., Kirkland, C.L., Van Kranendonk, M.J., Wyche, S., 2010. Age and significance of voluminous mafic–ultramafic magmatic events in the Murchison Domain, Yilgarn Craton. Aust. J. Earth Sci. 57, 597–614.

Jackson, S.E., Pearson, N.J., Griffin, W.L., Belousova, E.A., 2004. The application of laser ablation-inductively coupled plasma-mass spectrometry to in situ U-Pb zircon geochronology. Chem. Geol. 211, 47–69.

Kemp, A.I.S., Hawkesworth, C.J., Paterson, B.A., Kinny, P.D., Kemp, T., 2006. Episodic growth of the Gondwana supercontinent from hafnium and oxygen isotopes in zircon. Nature 439, 580–583.

Kemp, A.I.S., Shimura, T., Hawkesworth, C.J., 2007. Linking granulites, silicic magmatism, and crustal growth in arcs: ion micropobe (zircon) U-Pb ages from the Hidaka metamorphic belt, Japan. Geology 35, 807–810.

Kemp, A.I.S., Wilde, S.A., Hawkesworth, C.J., Coath, C.D., Nemchin, A., Pidgeon, R.T., Vervoort, J.D., DuFrane, S.A., 2010. Hadean crustal evolution revisited: new constraints from Pb-Hf isotope systematics of the Jack Hills zircons. Earth Planet. Sci. Lett. 296, 45–56.

Kirkland, C.L., Smithies, R.H., Woodhouse, A.J., Howard, H.M., Wingate, M.T.D., Belousova, E.A., Cliff, J.B., Murphy, R.C., Spaggiari, C.V., 2013. Constraints and deception in the isotopic record; the crustal evolution of the west Musgrave Province, central Australia. Gondwana Res. 23, 759–781.

Kirkland, C.L., Spaggiari, C.V., Wingate, M.T.D., Smithies, R.H., Belousova, E.A., Murphy, R., Pawley, M.J., 2011. Inferences on crust–mantle interaction from Lu–Hf isotopes: a case study from the Albany–Fraser Orogen. Rec. Geol. Surv. West. Aust. 12, 25.

Kohanpour, F., Kirkland, C.L., Gorczyk, W., Occhipinti, S., Lindsay, M.D., Mole, D., Le Vaillant, M., 2019. Hf isotopic fingerprinting of geodynamic settings: integrating isotopes and numerical models. Gondwana Res. 73, 190–199.

Lam, N.S.-N., 1983. Spatial interpolation methods: a review. Am. Cartogr. 10, 129–150.

Laurent, O., Zeh, A., 2015. A linear Hf isotope-age array despite different granitoid sources and complex Archean geodynamics: example from the Pietersburg block (South Africa). Earth Planet. Sci. Lett. 430, 326–338.

McCullagh, M.J., 1988. Terrain and surface modelling systems: theory and practice. Photogramm. Rec. 12, 747–779.

Meija, J., Coplen, T.B., Berglund, M., Brand, W.A., De Bièvre, P., Gröning, M., Prohaska, T., 2016. Atomic weights of the elements 2013 (IUPAC technical report). Pure Appl. Chem. 88, 265–291.

Milisenda, C.C., Liew, T.C., Hofmann, A.W., Kröner, A., 1988. Isotopic mapping of age provinces in Precambrian high-grade terrains: Sri Lanka. J. Geol. 96, 608–615.

Milisenda, C.C., Liewa, T.C., Hofmanna, A.W., Köhler, H., 1994. Nd isotopic mapping of the Sri Lanka basement: update, and additional constraints from Sr isotopes. Precambrian Res. 66, 95–110.

Mole, D.R., Fiorentini, M.L., Cassidy, K.F., Kirkland, C.L., Thebaud, N., McCuaig, T.C., Doublier, M.P., Duuring, P., Romano, S.S., Maas, R., Belousova, E.A., Barnes, S.J., Miller, J., 2015. Crustal evolution, intra-cratonic architecture and the metallogeny of an Archaean craton. In: Jenkin, G.R.T., Lusty, P.A.J., Mcdonald, I., Smith, M.P., Boyce, A.J., Wilkinson, J.J. (Eds.), Ore Deposits in an Evolving Earth, vol. 393. Geological Society of London, Special Publications, pp. 23–80.

Morel, M.L.A., Nebel, O., Nebel-Jacobsen, Y.J., Miller, J.S., Vroon, P.Z., 2008. Hafnium isotope characterization of the GJ-1 zircon reference material by solution and laser-ablation MC-ICPMS. Chem. Geol. 255, 231–235.

Nebel, O., Nebel-Jacobsen, Y., Mezger, K., Berndt, J., 2007. Initial Hf isotope compositions in magmatic zircon from early Proterozoic rocks from the Gawler Craton, Australia: a test for zircon model ages. Chem. Geol. 241, 23–37.

Nowell, G., Parrish, R.R., 2001. Simultaneous Acquisition of Isotope Compositions and Parent/daughter Ratios by Non-isotope Dilution-Mode Plasma Ionisation Multi-Collector Mass Spectrometry (PIMMS), vol. 267. Special Publication-Royal Society Of Chemistry. Royal Society of Chemistry, pp. 298–310.

Patchett, P.J., Vervoort, J.D., Söderlund, U., Salters, V.J.M., 2004. Lu–Hf and Sm–Nd isotopic systematics in chondrites and their constraints on the Lu–Hf properties of the Earth. Earth Planet. Sci. Lett. 222, 29–41.

Payne, J.L., McInerney, D.J., Barovich, K.M., Kirkland, C.L., Pearson, N.J., Hand, M., 2016. Strengths and limitations of zircon Lu-Hf and O isotopes in modelling crustal growth. Lithos 248–251, 175–192.

Plank, T., 2005. Constraints from thorium/lanthanum on sediment recycling at subduction zones and the evolution of the continents. J. Petrol. 46, 921–944.

Puetz, S.J., Condie, K.C., 2019. Time series analysis of mantle cycles part I: periodicities and correlations among seven global isotopic databases. Geosci. Front. 10 (4), 1305–1326.

Roberts, N.M.W., Slagstad, T., Parrish, R.R., Norry, M.J., Marker, M., Horstwood, M.S.A., 2013. Sedimentary recycling in arc magmas: geochemical and U–Pb–Hf–O constraints on the Mesoproterozoic Suldal Arc, SW Norway. Contrib. Mineral. Petrol. 165, 507–523.

Roberts, N.M.W., Spencer, C.J., 2015. The zircon archive of continent formation through time, 389. Geological Society, London, Special Publications, pp. 197–225.

Salters, V.J.M., Stracke, A., 2004. Composition of the depleted mantle. Geochem. Geophys. Geosyst. 5.

Scherer, E., Münker, C., Mezger, K., 2001. Calibration of the lutetium-hafnium clock. Science Am. Assoc. Adv. Sci. 293, 683–687.

Sláma, J., Košler, J., Condon, D.J., Crowley, J.L., Gerdes, A., Hanchar, J.M., Horstwood, M.S.A., Morris, G.A., Nasdala, L., Norberg, N., Schaltegger, U., Schoene, B., Tubrett, M.N., Whitehouse, M.J., 2008. Plešovice zircon - a new natural reference material for U-Pb and Hf isotopic microanalysis. Chem. Geol. 249, 1–35.

Söderlund, U., Patchett, P.J., Vervoort, J.D., Isachsen, C.E., 2004. The ^{176}Lu decay constant determined by Lu-Hf and U-Pb isotope systematics of Precambrian mafic intrusions. Earth Planet. Sci. Lett. 219, 311–324.

Spencer, C.J., Danišík, M., Ito, H., Hoiland, C., Tapster, S., Jeon, H., McDonald, B., Evans, N.J., 2019a. Rapid exhumation of earth's youngest exposed granites driven by subduction of an oceanic arc. Geophys. Res. Lett. 1–9.

Spencer, C.J., Dyck, B., Mottram, C.M., Roberts, N.M.W., Yao, W.H., Martin, E.L., 2019b. Deconvolving the pre-Himalayan Indian margin – tales of crustal growth and destruction. Geosci. Front. 10, 863–872.

Spencer, C.J., Kirkland, C.L., Prave, A.R., Strachan, R.A., Pease, V., 2018. Crustal reworking and orogenic styles inferred from zircon Hf isotopes: Proterozoic examples from the North Atlantic region. Geosci. Front. 10, 417–424.

Spencer, C.J., Kirkland, C.L., Taylor, R.J.M., 2016. Strategies towards statistically robust interpretations of in situ U-Pb zircon geochronology. Geosci. Front. 7, 581–589.

Spencer, C.J., Yakymchuk, C., Ghaznavi, M., 2017. Visualising data distributions with kernel density estimation and reduced chi-squared statistic. Geosci. Front. 8, 1247–1252.

Tang, M., Wang, X.-L., Shu, X.-J., Wang, D., Yang, T., Gopon, P., 2014. Hafnium isotopic heterogeneity in zircons from granitic rocks: geochemical evaluation and modeling of "zircon effect" in crustal anatexis. Earth Planet. Sci. Lett. 389, 188–199.

Thirlwall, M.F., Walder, A.J., 1995. Situ hafnium isotope ratio analysis of zircon by inductively coupled plasma multiple collector mass spectrometry. Chem. Geol. 122, 241–247.

Vermeesch, P., 2012. On the visualisation of detrital age distributions. Chem. Geol. 312–313, 190–194.

Vervoort, J.D., Blichert-Toft, J., 1999. Evolution of the depleted mantle: Hf isotope evidence from juvenile rocks through time. Geochem. Cosmochim. Acta 63, 533–556.

Vervoort, J.D., Kemp, A.I., Fisher, C.M., 2018. Hf Isotope Constraints on Evolution of the Depleted Mantle and Growth of Continental Crust. AGU Fall Meeting Abstracts.

Vervoort, J.D., Kemp, A.I.S., 2016. Clarifying the zircon Hf isotope record of crust – mantle evolution. Chem. Geol. 425, 65–75.

Vervoort, J.D., Patchett, P.J., Blichert-toft, J., Albare, F., 1999. Relationships between Lu – Hf and Sm – Nd isotopic systems in the global sedimentary system. Earth Planet. Sci. Lett. 168, 79–99.

Villaros, A., Stevens, G., Buick, I.S., 2009. Tracking S-type granite from source to emplacement: clues from garnet in the cape granite suite. Lithos 112, 217–235.

Wang, Q., Wilde, S.A., 2018. New constraints on the Hadean to Proterozoic history of the Jack Hills belt, western Australia. Gondwana Res. 55, 74–91.

Watson, D., 1999. The natural neighbor series manuals and source codes. Comput. Geosci. 25, 463–466.

White, W.M., Patchett, J., 1984. HfNdSr isotopes and incompatible element abundances in island arcs: implications for magma origins and crust-mantle evolution. Earth Planet. Sci. Lett. 67, 167–185.

Woodhead, J.D., Hergt, J.M., 2005. A preliminary appraisal of seven natural zircon reference materials for in situ Hf isotope determination. Geostand. Geoanal. Res. 29, 183–195.

Wu, F.-Y., Yang, Y.-H., Xie, L.-W., Yang, J.-H., Xu, P., 2006. Hf isotopic compositions of the standard zircons and baddeleyites used in U–Pb geochronology. Chem. Geol. 234, 105–126.

Wyche, S., Kirkland, C.L., Riganti, A., Pawley, M.J., Belousova, E., Wingate, M.T.D., 2012. Isotopic constraints on stratigraphy in the central and eastern Yilgarn Craton, Western Australia. Aust. J. Earth Sci. 59, 657–670.

Xu, P., Wu, F., Xie, L., Yang, Y., 2004. Hf isotopic compositions of the standard zircons for U-Pb dating. Chin. Sci. Bull. 49, 1642–1648.